



Quasar absorption lines: an overview

Pushpa Khare*

CSIR Emeritus Scientist, IUCAA, Pune, India

Received 2013 March 10; accepted 2013 March 29

Abstract. Quasar spectra, apart from showing the broad, redshifted emission lines, often show narrow as well as broad absorption lines. The presence of absorption lines has been known since shortly after the discovery of these objects. The spectrum of a single quasar can have more than one group of absorption lines, termed absorption line systems, each system having its characteristic redshift. Most of these systems are believed to be produced by galactic or intergalactic clouds, while those having redshifts close to that of the quasar may be produced by material intrinsic to the quasar. These systems thus offer a sensitive probe to understand the evolutionary history of the Universe over 90% of its age as well as the quasar environment. In recent times, the commissioning of large telescopes, high resolution spectrographs, space telescopes, large sky digital surveys and progress in hydro-simulations have resulted in rapid progress in this field. In this article, I will summarize some of our current understanding of these systems and the information that has been obtained about various aspects of the Universe from their study.

Keywords : quasars: absorption lines – quasars: general – intergalactic medium

1. Introduction

Radiation from distant quasars interacts with the material lying along its path before it reaches the observer. The signatures of these interactions can be discerned from the observed quasar spectrum. The evidence of the interactions is the reduction in the number of photons at wavelengths specific to the interacting material in the form of absorption lines, reddening of the spectrum, and the 2175 Å bump in the rest frame of the absorber. In some cases, emission from the intervening material is also seen. Quasar absorption lines were discovered soon after the discovery of the first quasar. Thus, quasar spectra are store houses of vast amount of information about the interstellar medium in the intervening galaxies as well about the intergalactic medium (IGM).

*email: pushpakhare@gmail.com

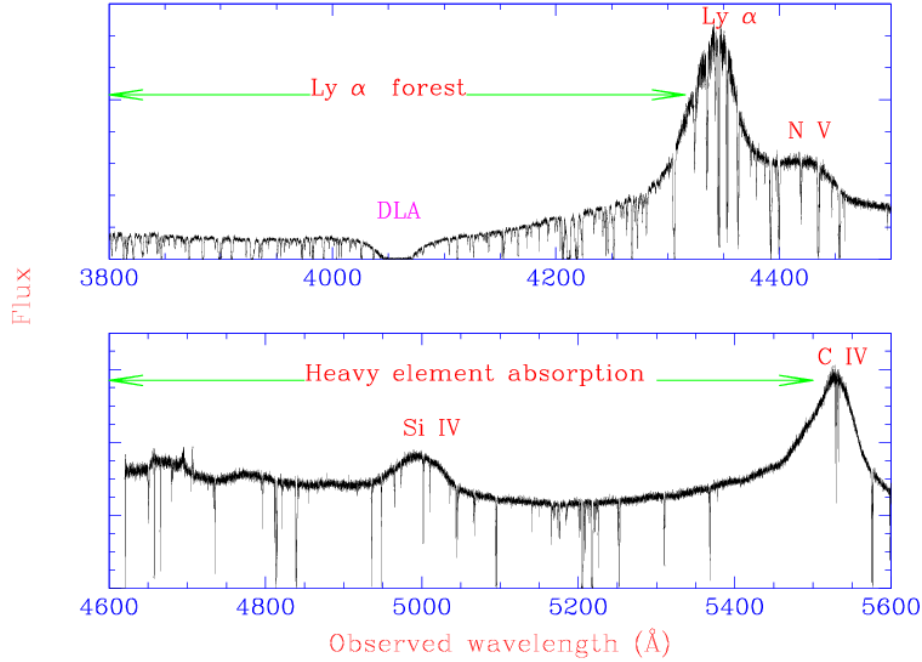


Figure 1. Typical spectrum of a quasar with emission redshift of ~ 2.6 , showing the quasar continuum, emission lines (labeled), and a number of absorption lines. The quasar has a Damped Lyman Alpha system (discussed below) with redshift ~ 2.3 in its spectrum. The absorption lines long-wards of Lyman alpha emission are produced by heavy elements mostly in galactic interstellar clouds, while most of those on the shorter wavelength side are due to neutral hydrogen in intergalactic clouds.

A typical quasar spectrum shows broad emission lines with widths of several thousands of km s^{-1} superimposed on a power-law spectrum. In addition it often has several narrow absorption lines, as noted above, with widths ranging from a few tens to a few hundreds of km s^{-1} . A typical quasar spectrum is shown in Fig. 1. A careful examination of the absorption lines on the long wavelength side of the Ly α emission line, reveals that these lines fall into distinct groups, each group having several lines of heavy elements, at a particular (absorption) redshift, z_{abs} . Typical lines are of C IV, Mg II, Si IV, C II, Si II, Fe II etc. Each group of lines constitutes an absorption system. The H I lines belonging to these systems are also seen if they fall in the observable window. Several absorption systems, each having a distinct absorption redshift, are often found in the spectra of a single quasar. Most absorption systems have the absorption redshift smaller than the emission redshift, z_{em} .

Most of the large number of lines on the short wavelength side of the Ly α emission line can

not be identified with any of the heavy element lines and these are believed to be Ly α lines at different redshifts, forming what is called the Ly α forest.

The absorption systems are divided into various classes, essentially based on N_{HI} , the H I column density in the absorbers. The two strongest among these classes, having $N_{\text{HI}} \geq 2 \times 10^{20} \text{ cm}^{-2}$ and N_{HI} between 10^{19} cm^{-2} and $2 \times 10^{20} \text{ cm}^{-2}$, are called damped Ly α (DLA) and sub-damped Ly α (sub-DLA) systems respectively and are believed to contain most of the neutral gas at high redshifts (Prochaska, Herbert-Fort & Wolfe 2005). Systems with N_{HI} between 2×10^{17} and 10^{19} cm^{-2} are called Lyman Limit Systems (LLS) as these systems have sufficient H I to completely absorb the ionizing radiation of the background quasar and cause a sharp break in its spectrum at the Lyman Limit (912 Å) in the rest-frame of the system. The DLA and sub-DLA systems can also be considered to be LLS. Ly α forest systems usually have H I column smaller than that of the LLS. Doublet lines of Mg II or C IV are easily identified and systems having these lines are also termed as Mg II or C IV systems respectively, particularly in cases when either their redshifts do not allow the Ly α line to be seen in the optical region or the resolution of the spectrum does not allow accurate determination of H I column density.

A few quasars show very broad (with velocities of several thousands of km s^{-1}) absorption lines at redshifts close to that of the quasar, giving rise to the nomenclature ‘BAL’ (Broad Absorption Line) systems/quasars. These are believed to be produced by material thrown out by the quasars and are intrinsic to the quasar. In some cases narrow lines at redshifts very close to the emission redshift (called the associated systems) are too numerous to be intervening and some of these could be produced by material associated with the quasar. Rest of the absorption lines are believed to be formed by gaseous material in intervening galaxies or in IGM, lying along the line-of-sight to the quasar. This belief arises from (Sargent et al. 1980) the (i) energetic arguments: huge amounts of energy, too large to be realistic, would be necessary to produce the observed relative velocities indicated by the redshift differences between the emission and absorption redshifts, if the absorbing material were ejected by the quasar (ii) lack of correlation between properties of absorption lines and those of the quasar itself, (iii) the close to Poissonian distribution of absorption redshifts, and (iv) the direct observation by deep imaging of several galaxies lying close to the line-of-sight (e.g. Bergeron 1988; Zwaan et al. 2005) at the redshift of absorption systems.

Quasar absorption line systems (QSOALS) thus provide a very sensitive (as minute traces of gas with column densities as small as 10^{11} cm^{-2} can be measured) and unbiased tool to study the IGM and intervening galaxies irrespective of their morphology, brightness, size etc, at redshifts up to the highest redshift of the observed quasars which is ~ 7 . This covers $\sim 94\%$ of the age of the Universe. Studies of QSOALS have provided valuable information about various aspects of the Universe, including the large scale structure, structure formation history and nucleosynthesis details, strength, nature and evolution of the UV background radiation field, abundance and nature of dust in the absorbers, quasar outflows, chemical enrichment history of the Universe, cosmic microwave background radiation (CMBR) temperature at high redshifts, variation of the fundamental constants etc.

Large, homogeneous samples of QSOALS taken at high or intermediate resolution, are necessary to determine their statistical properties e.g. the number density, equivalent width and column density distributions, clustering, the average properties of the absorbers like the dust content and chemical abundances and their evolution with redshift. These can then be compared with predictions of structure formation models. One of the early large sample studies was conducted by Steidel & Sargent (1989; 1992) who observed about 100 quasars and determined the statistical properties of QSOALS. By comparing these with the number density of galaxies, the sizes of the galaxies were estimated to be several tens of kpc, which was consistent with galactic halo origin of the absorption systems as was postulated by Bahcall & Spitzer (1969). Larger, albeit inhomogeneous samples consisting of several hundred quasars were compiled by several authors (e.g. York et al. 1991; Vanden Berk et al. 1996).

A very large and homogeneous sample has recently become available thanks to the Sloan Digital Sky Survey (SDSS) (York et al. 2000). The SDSS Data Release 9 (DR9) has the spectra of 228,468 quasars, observed at a resolution of 1700–2000, covering a wavelength range of 3800–9200 Å. This has led to a revolution in QSOALS studies and has led to a deeper understanding of the Universe.

Below, I have tried to summarize some of the recent results in this field, starting with a brief history. In a review of this size, it is not possible to cover all aspects of the subject and some subjectivity does creep in, with bias towards the topics one is interested in, in spite of conscious efforts to be neutral. Also, it is not possible to go into details of the topics. I therefore, apologize for the sketchiness of the description. I have tried to give references, both old and recent, which may help the readers to follow the topics covered here, in more details. Also, interested readers may refer to more detailed reviews on the topic (e.g. Rauch 1998; Wolfe, Gawiser & Prochaska 2005; Meiksin 2009).

2. Studies of Ly α forest

The first systematic survey for the forest lines was carried out by Sargent et al. (1980). On the basis of their number density (which was too large to have been produced by galaxies) they concluded that the lines are mostly of intergalactic origin. Some of these could possibly originate in the outer halos of galaxies (Lanzetta et al. 1995; Prochaska et al. 2011). Studies of these lines provide an understanding of the distribution of and physical conditions in the IGM and hence are probes of structure formation at high redshifts.

2.1 Ly α absorber models

Early studies of the forest concentrated on determining their number density and column density distributions as a function of redshift which could then be matched with the predictions of theoretical models. Early models of the forest absorbers included pressure confined intergalactic clouds (e.g. Sargent et al. 1980), baryons in dark matter mini-halos (e.g. Rees 1986), caustics and sheets produced by growth of gravitational perturbation (e.g. Meiksin 1994), outflows from

galaxies (Wang 1995), pressure confined clouds inside halos of galaxies (Mo & Miralda-Escude 1996) etc. Semianalytic hierarchical models of structure formation, using Press-Schechter prescription for mass function of halos were considered to understand the observed distribution of various properties of different classes of QSOALS (e.g. Mo & Morrison 1994; Das & Khare 1999).

The semianalytic models were soon replaced by numerical cosmological simulations. These showed that the IGM fragments into an interconnected network of sheets, filaments and halos. Ly α lines in the redshift (z) range of 2–5 are caused by mildly overdense photoionized intergalactic gas which closely traces the dark matter distribution in the filaments and sheets in the cold dark matter universe. Being mildly non-linear, their properties can be well predicted by the simulations using simulated spectra. These are sensitive to the cosmological parameters used which can be constrained by a comparison with observations (e.g. Bi & Davidson 1997; Jena et al. 2005). The Baryonic Oscillation Spectroscopic Survey (BOSS) will observe Ly α forest in the spectra of 150,000 quasars with g magnitude smaller than 22, over the redshift range of 2.15–3.5 (Dawson et al. 2013) which will constrain cosmological parameters to high accuracy.

2.2 Chemical enrichment of the IGM

Initially the IGM producing the forest lines was believed to be pristine, devoid of metals. However, with higher resolution, higher signal-to-noise spectra, heavy element lines were found to accompany stronger hydrogen lines in the spectra of quasars with redshifts of 2–3 (Cowie et al. 1995). It is believed from the observed correlations between galaxies and intergalactic C IV absorption lines at z between 1.5 to 3.5, that outflows from galaxies are responsible for contaminating the IGM (Adelberger 2005). Simcoe (2011) has determined carbon abundance in IGM at z between 4 and 4.5 using 131 Ly α absorbers with $\log(N_{\text{HI}}) > 14.5$ to be $[\text{C}/\text{H}] = -3.55$. Comparing this with the abundance in similar absorbers at lower redshifts, they find that that $\sim 50\%$ of the heavy elements seen in the intergalactic medium at $z \sim 2.4$ were deposited in the 1.3 Gyr between $z \sim 4.3$ and $z \sim 2.4$. The total implied mass fraction of carbon into the Ly α forest would constitute $\sim 30\%$ of the initial mass function weighted carbon yield from known star-forming populations over this period. The buildup of chemical abundances in the IGM can thus provide constraints on outflow mechanisms and star formation history of the Universe.

2.3 Opacity of Ly α forest

Properties of Ly α forest lines at $z < 1.6$ were compiled by Kirkman et al. (2007) using HST spectra of 74 quasars. They find a slow variation with redshift of the mean absorption; $DA(z) = 1 - F(z) = 0.016(1 + z)^{1.01}$, $F(z)$ being the average transmitted flux. This has been found to be consistent with the predictions of large hydrodynamic simulations (Paschos et al. 2009). At high redshifts, $2 < z < 5$, a large sample of Ly α forest lines in 6065 quasars from SDSS DR7 has been used by Becker et al. (2013), to determine the mean transmitted flux using the

method of composite spectra. They find the mean transmission ($e^{-\tau(z)}$) to vary smoothly with z as $\tau(z)[(1+z)/(1+z_0)]^\beta + C$, with $[\tau_0, \beta, C] = [0.751, 2.90, 0.132]$, for $z_0 = 3.5$. The smooth variation indicates a continuous variation of H I ionizing radiation and IGM temperatures with redshift.

2.4 Proximity effect and background UV radiation field

The strong UV field of quasars ionizes the nearby Ly α absorbers, causing a depletion in the number of Ly α absorption lines above a given N_{HI} close to the quasar redshifts. This is termed the (line-of-sight) proximity effect and can be used to determine (Bajtlik, Duncan & Ostriker 1988; Calverley et al. 2011) the background UV radiation field through a comparison of the distribution of Ly α forest lines around quasars with their distribution away from the quasars at similar redshifts. Initially, the calculations did not take into account the matter overdensities in regions around quasars, thereby overestimating the UV background (Loeb & Eisenstein 1995). Rollinde et al. (2005), using the UV background flux to be that inferred from the mean Ly α opacity in the forest region at $z \sim 2$ to 3, concluded that an over density of the order of a few near the quasars is necessary to explain the observations. The extent of transverse proximity effect due to a quasar lying close to the line-of-sight of another quasar has been used to put constraints on the lifetime of quasars which was found to be surprisingly low $\sim 10^6$ yr (e.g. Kirkman & Tytler 2008). Lu & Yu (2011) using a large number of Monte Carlo generated synthetic Ly α forest spectra showed that the quasar properties and environment can be constrained simultaneously by considering the transverse and the line-of-sight proximity effects of bright type 1 quasars together. The current available observations suggest that the density is significantly enhanced in the vicinity of the quasars and that quasar lifetime is consistent with being as large as a few 10^7 yr.

2.5 Ly α absorbers and voids at low redshifts

A significant excess at high confidence levels of Ly α systems at $z < 0.1$, at the edges of galaxy voids with respect to a random distribution, on $\sim 5h^{-1}$ Mpc scales has been found by Tejos et al. (2012). They find no significant difference in the number of systems inside voids with respect to the random expectation and report differences between both N_{HI} and Doppler parameter (b_{HI}) distributions of Ly α systems found inside and at the edge of galaxy voids. Low-density environments (voids) have smaller values for both N_{HI} and b_{HI} than higher density ones (edges of voids). These trends are theoretically expected and also found in Galaxies-Intergalactic Medium Interaction Calculation which is a state-of-the-art hydrodynamical simulation.

2.6 Gunn–Peterson effect and epoch of reionization of the Universe

Gunn & Peterson (1965) derived the fraction of neutral hydrogen in IGM from the detection of flux short-wards of the Ly α emission line in a quasar spectrum. Since then, the method is used to

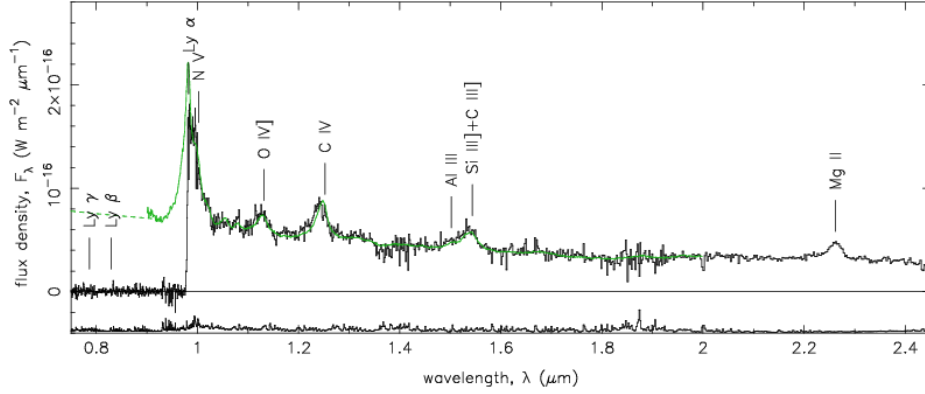


Figure 2. Spectrum of ULAS J1120+0641 and a composite spectrum, shown in green, derived from lower redshift quasars. The H I absorption wing towards the short wavelength side of the Ly α peak is evident. Courtesy Mortlock et al. (2011) *Nature*, 474, 616.

measure the epoch of reionization of the Universe using high redshift ($z \gtrsim 6$) quasars discovered by the SDSS. Fully black Gunn–Peterson troughs have been found in a number of $z > 6$ SDSS quasars, as well as in the quasar ULAS J1120+0641 recently discovered at $z = 7.085$ (Mortlock et al. 2011) in the UKIRT Infrared Deep Sky Survey, which is shown in Fig. 2. However, calculations show that a neutral fraction as low as 10^{-4} in a patch of the IGM is sufficient to produce a black Gunn–Peterson trough. The reionization epoch is believed to have been at redshifts between 6 and 15. Recent analysis of 3, $z > 6$ quasars, assuming a patchy IGM (Schroeder, Messinger & Heiman 2013) supports the reionization to be incomplete at redshifts ~ 6 to 7. This has important implications for the structure formation models.

2.7 Baryon content in the IGM

Hydrodynamic simulations of structure growth have suggested (Cen et al. 1995) that a large fraction of baryons at the present epoch may be in a gaseous phase with temperatures $\sim 10^5$ – 10^7 K (called the warm hot phase of the IGM or WHIM) at moderate overdensities of typically ~ 10 to 40. The O VI $\lambda\lambda 1032, 1038$ absorption lines are ideal for observing this gas. HST observations indeed detected this gas (Tripp, Savage & Jenkins 2000). WHIM has also been observed at high redshifts through the O VI and Ne VIII lines (e.g. Tripp 2013). Muzahid et al. (2012) have studied a sample of 84 O VI systems at $z \sim 2.3$. They find $\Omega_{\text{O VI}} \geq (1.0 \pm 0.2) \times 10^{-7}$ for $\log(N_{\text{O VI}}) > 13.7$ and that roughly 2.8% baryons reside in the O VI phase at these redshifts. O VI lines could be produced by collisionally ionized gas as well as photoionized gas at low densities. On the other hand, Ne VIII lines can only be produced by gas in collisional equilibrium peaking at 7×10^5 K. The observation of these lines thus gives insights into the thermal state of the IGM.

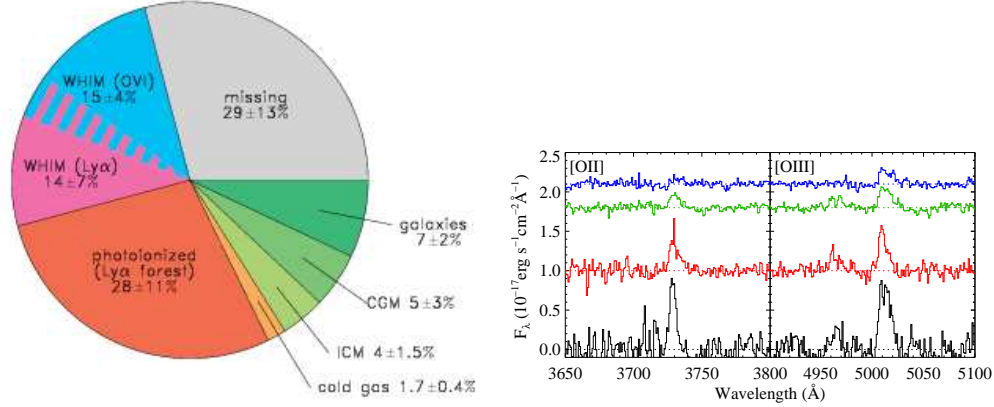


Figure 3. Left Panel: Compilation of current observational measurements of the low redshift baryon census. Slices of the pie chart show baryons in collapsed form, in the circumgalactic medium (CGM) and intercluster medium (ICM), and in cold gas (H I and He I). Primary baryon reservoirs include diffuse photoionized Ly α forest and WHIM traced by O VI and broad Ly α absorbers. Blended colours (BLAs and O VI) have a combined total of $25\% \pm 8\%$, smaller than their direct sum (17% plus 14%) owing to corrections for double-counting of WHIM at 10^5 – 10^6 K with detectable metal ions. Courtesy Shull et al. (2012) ApJ, 759, 23. Right Panel: [O II] (left) and [O III] (right) emission lines from stacking quasar spectra with intervening Mg II absorbers at $0.5 < z_{\text{abs}} < 0.7$ with different Mg II $\lambda 2796$ rest equivalent widths. From top to bottom: $W_{\text{Mg II}} < 1$; $1 \leq W_{\text{Mg II}} < 2$; $2 \leq W_{\text{Mg II}} < 3$; $W_{\text{Mg II}} \geq 3$ Å. The continuum-subtracted spectra are shifted vertically by a constant for display purpose. Courtesy Noterdaeme et al. (2010) MNRAS, 403, 906.

Recent analysis (Komatsu et al. 2011) of the spectrum of acoustic peaks in the CMBR obtained by the Wilkinson Microwave Anisotropy Probe found that baryons comprise a fraction $\Omega_b = 0.0455 \pm 0.0028$ of the critical matter–energy density of the Universe. At low z , substantial baryon fractions are present in the photoionized Ly α forest ($28\% \pm 11\%$) and WHIM traced by O VI and broad-Ly α absorbers (BLAs; having widths of $> 40 \text{ km s}^{-1}$) ($25\% \pm 8\%$). The collapsed phase (galaxies, groups, clusters, circum-galactic-medium) contains $18\% \pm 4\%$, leaving an apparent baryon shortfall of $29\% \pm 13\%$. These may be present in hotter phase of the IGM and in weaker Ly α and O VI absorbers (Shull, Smith & Danforth 2012). Simulations suggest that about 15% may be residing in X-ray-absorbing gas at $T \sim 10^{6.3}$ K. The baryon census of the Universe is shown in the left panel of Fig. 3.

2.8 He II forest

Lines of He II from the IGM were first detected by Jakobsen et al. (1994) using the HST. Observations by the Far Ultraviolet Spectroscopic Explorer (FUSE) have revealed the presence of He II Ly α forest (e.g. Shull et al. 2004). The reionization epoch of He II (ionized to He III) is believed to have lagged behind the reionization epoch of H I (at $z > 6$) because of the lack of high energy

photons in galactic spectra and to have been completed around $z \sim 2.7$ when such photons were available in sufficient quantities from the quasars (Wyithe & Loeb 2003). Large He II opacity fluctuations have been observed along several lines of sight (e.g. Gabor et al. 2011), some of which could be due to transverse proximity effect (Jakobsen et al. 2003).

3. Broad Absorption Line quasars (BAL quasars)

About 10–20 % of quasars are classified as BAL quasars (Weyman, Carswell & Smith 1981). Their broad absorption lines usually occur at redshifts close to those of the quasars and are believed to be caused by material flowing out of the quasars. BALs with highly relativistic speeds of 0.1c to 0.2c with respect to the quasar have been observed (Hamann et al. 2013). HiBAL quasars are BAL quasars which are observed in high ionization lines like C IV $\lambda 1550$ and Si IV $\lambda 1400$ without corresponding absorption in low ions. Those also showing absorption from low ions of Mg II $\lambda 2800$ are less common and are termed LoBALs. Even rarer are those BAL quasars which also show BALs from one or more species of iron and are termed FeLoBALs. Radiation pressure from the quasars is believed to be the cause of the outflow. The material causing absorption has to be shielded by highly ionized and radiatively thick layer of material which causes strong absorption at X-ray wavelengths (Gallagher et al. 2006). Some models assume the BAL phenomenon to be the effect of orientation while some others assume this to be an evolutionary stage of the quasars. From a study of a sample of 3547 SDSS HiBALs, Allen et al. (2011) find the BAL fraction to have decreased by a factor of 3.5 from $z = 4$ to $z = 2$. Strong variability is often seen in these quasars (Vivek et al. 2012).

4. Heavy element systems

4.1 Mg II systems

As noted above, Mg II systems being easily identifiable in optical spectra at redshifts smaller than 2, and being abundant, have been the subject of a large number of studies starting in the late seventies and continuing till date. Average abundance of 370 strong Mg II systems with rest equivalent width of Mg II $\lambda 2796$ ($W_{\text{Mg II}} > 1.0 \text{ \AA}$), at redshifts between 0.9–2.0, in the Early Data Release (EDR) sample was determined by Nestor et al. (2003) by constructing an arithmetic mean composite spectrum in the absorber rest frame. They found $[\langle Z \rangle / \langle H \rangle] = -1.13 \pm 0.19$. Nestor, Turnshek & Rao (2005) studied the redshift and equivalent width distributions of 1300 Mg II systems with $W_{\text{Mg II}} > 0.3 \text{ \AA}$ in EDR at redshifts between 0.37 and 2.27. They found the $W_{\text{Mg II}}$ distribution to be well fitted by two exponentials indicating that the Mg II absorbers consist of two distinct populations. A large sample of $\sim 17,000$ Mg II systems with $0.36 < z_{\text{abs}} < 2.28$ has been compiled by Quider et al. (2011) from SDSS DR4 and has been used for several investigations, some of which have been reported here.

There are two hypothesis regarding the nature of these systems. There are reasons to believe that these systems could be formed by cool clumps embedded in hot galactic outflows.

With the aim of detecting absorbing galaxies, Zibetti et al. (2005) stacked SDSS images of 700 quasars having absorption systems with $W_{\text{Mg II}} > 0.8 \text{ \AA}$ and found an excess of brightness around the line-of-sight at 6σ level. The outflow hypothesis is supported by the correlation between Mg II equivalent widths and star formation rates in the absorbing galaxies as measured from the [O II] $\lambda 3727$ flux (Noterdaeme, Srianand & Mohan, 2010; Menard et al. 2011). The right panel of Fig. 3 shows the [O II] $\lambda 3727$ and [O III] $\lambda\lambda 4959, 5007$ emission lines in the continuum subtracted composite spectra of samples of Mg II systems in 46 SDSS DR7 quasars which show emission from the host galaxy, in different $W_{\text{Mg II}}$ bins.

This view has been challenged by Chen et al. (2010) who find little evidence for correlation between absorber strength and galaxy colours using a galaxy-selected sample of Mg II systems, albeit for weaker systems. These and other studies of the inclination of absorbing galaxies seem to indicate that weaker systems ($W_{\text{Mg II}} < 1 \text{ \AA}$) are more likely to be infalling in the plane of the disc, while the stronger systems arise in outflows perpendicular to the disc. Recently, Matejek et al. (2013) studied a large sample of Mg II systems at high redshifts ($1.98 < z_{\text{abs}} < 5.33$) using infrared observations. At high redshifts ($\langle z_{\text{abs}} \rangle = 3.4$), they find all Mg II systems to be sub-DLAs or DLAs, the DLA fraction being > 2.5 times that at lower redshifts ($\langle z_{\text{abs}} \rangle = 0.9$). The sub-DLAs (associated with $W_{\text{Mg II}}$ between 0.3 and 1 \AA) are found to be have high metallicity ~ 0.1 solar. It is suggested that if the weaker systems are indeed infalling material, it must be the reaccreting material which was earlier ejected by the galaxy.

4.2 C IV systems

A large sample of 14722 C IV systems covering a redshift range of 1.46 to 4.55 has been compiled from SDSS DR7 by Cooksey et al. (2013). The equivalent width distribution has been found to be an exponential with little evolution in the shape with redshift. The comoving number density is seen to have increased by more than a factor of two between redshifts of 4.55 and 1.96, below which it remains constant. Low and high redshift data from the literature seems to indicate a ten fold increase in the number density of C IV systems between redshifts of 6 and 0.

4.3 Damped Lyman Alpha systems

Rao & Turnshek (2000) and Rao, Turnshek & Nestor (2006) measured the H I column densities of about 200 strong Mg II ($W_{\text{Mg II}} > 0.3 \text{ \AA}$) systems at redshifts < 1.65 from observations of their UV spectra using HST, and studied statistical properties of DLAs found therein. They found the incidence of DLAs per unit redshift per line-of-sight to be about $0.044(1+z_{\text{abs}})^{1.27}$. Prochaska et al. (2005) studied the properties of DLAs at redshifts between 1.6 and 3.5 in SDSS DR3. They made an interesting observation that there are about 40% more DLAs towards bright quasars, which they concluded to be due to the lensing of quasars by the DLA absorbers. They also concluded that more than 80% of the neutral mass density in this redshift range is contributed by DLAs. Prochaska, Hennawi & Herbert-Fort (2008) found evidence for proximity effect i.e. the ionization of the absorbers proximate to the quasars due to their intense radiation fields, in DLAs by studying their distribution near the quasars.

Noterdaeme et al. (2012b) have compiled a sample of 12081 systems with $\log(N_{\text{HI}}) > 20$ with redshifts between 2.15 and 5.2 in SDSS DR9. The column density distribution, shown in the left panel of Fig. 4, is best fitted with a double power law (with slopes of -1.6 and -3.5) as well as a gamma function. The right panel of Fig. 4 shows the contribution of QSOALS to the cosmic neutral gas density as a function of N_{HI} . Maximum contribution seems to come from systems with N_{HI} around 10^{21} cm^{-2} . Left panel of Fig. 5 shows the evaluated cosmological mass density of neutral gas in DLAs. This decreases with redshift from 3.2 to 2.2; the value at $z = 2.2$ being twice that at $z = 0$. At $z \sim 3$ the value is found to be $\sim 10^{-3}$ which implies that neutral gas accounts for only 2% of baryons at these redshifts confirming that most of the baryons are in the form of ionized gas in IGM.

4.4 Dust content of the quasar absorbers

Early evidence for the presence of dust in DLAs was given by Pei, Bechtold & Fall (1991) by comparing the spectra of 13 quasars with DLAs in their spectra, with those of 15 quasars without DLAs; the quasars with DLAs being redder than those without DLAs. Presence of dust is also indicated by negative values of $[\text{Cr}/\text{Zn}]$ in DLAs. The 2175 Å feature has also been detected in a handful of absorbers, e.g. Srianand et al. (2008a), Jiang et al. (2011). The large sample of quasars provided by SDSS was used by Murphy & Liske (2004) for studying dust reddening by DLA absorbers. From a study of spectral indices of quasars with DLAs in SDSS DR2, at redshifts ~ 3 , they concluded that the DLAs have little dust with $E(B - V)$ values < 0.02 .

York et al. (2006) and Vanden Berk et al. (2008) have studied large samples of strong Mg II ($W_{\text{Mg II}} > 0.3 \text{ \AA}$) intervening and associated systems taken from SDSS DR1 and DR3 respectively. Their absorber samples for the two types of systems contained 809 and 415 Mg II systems with redshifts between 1 and 1.86. For each absorber sample, they constructed a non-absorber sample of the same number of quasars without any absorption system in their spectra and having emission redshift and i magnitude matching ($\Delta z_{\text{em}} < 0.1$ and $\Delta m_i < 0.2$) with the quasars in the absorber sample on a one to one basis, to avoid selection effects.

The extinction curves obtained by comparing the geometric mean composite spectra of the absorber and corresponding non-absorber samples (and sub-samples thereof) were found to be of SMC type (with no evidence of the 2175 Å bump) and yielded $E(B - V)$ values up to 0.085, amount of dust being dependent on the absorber properties. Definite evidence of dust in Mg II absorbers was thus obtained. The right panel of Fig. 5 shows the results for the sample of 251 intervening systems, having $W_{\text{Mg II}} > 2.5 \text{ \AA}$. Wild and Hewitt (2005) found strong Ca II absorbers to have LMC-type dust. Extinction in associated absorbers was found to be significantly higher than in intervening systems and among the associated systems, for radio loud quasars (Vanden Berk et al. 2008; Khare et al. 2013).

Khare et al. (2012) used the method of composite spectra to determine the dust content of a sample of 1084 DLAs in SDSS DR7 at $2.15 \leq z_{\text{abs}} \leq 5.2$. Dust was found to be present, albeit in very low quantities ($E(B - V) < 0.03$).

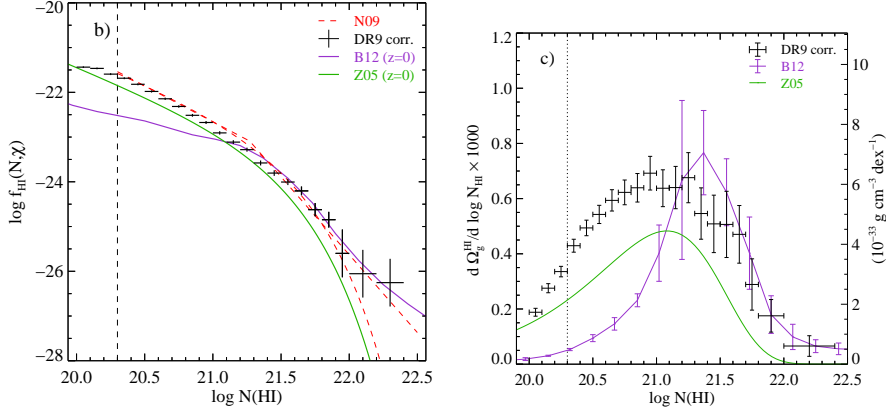


Figure 4. Left Panel: Column density distribution functions of N_{HI} at $z_{\text{abs}} = 2.5$. Horizontal bars represent the bin over which $f(N_{\text{HI}})$ is calculated and vertical error bars represent Poissonian uncertainty. The double power-law and Γ -function fits to the DR7 distribution (Noterdaeme et al. 2009; N09), are shown as red dashed lines. $f(N_{\text{HI}})(z = 0)$ are taken from Braun (2012, purple) and Zwaan et al. (2005, green). Courtesy Noterdaeme et al. (2012b) A&A, 547, L1. Right Panel: Contribution of DLAs in a given N_{HI} range to the total mass census of neutral gas. DR9 values are corrected for systematics. Courtesy Noterdaeme et al. (2012b), A&A, 547, L1.

4.5 Outflows from quasars

The presence of excess number of absorbers near the quasars, over that expected from the distribution of intervening galaxies was known since the late 1970s (e.g. Weymann et al. 1979). The excess absorbers could result from the interstellar medium in host galaxies, the galaxies clustering around quasars or material out-flowing from the quasars. Wild et al. (2008) have studied this excess using $\sim 16,000$ Mg II and ~ 7000 C IV systems in SDSS DR3. They estimated the clustering of absorbers around quasars from the 3D correlation between absorbers and quasars using close pairs of quasars. Taking into account the clustered component and the proximity effect they fitted the observed absorber distribution as a function of relative velocity with respect to the quasars. Their plot of the number density of C IV absorbers as a function of comoving distance from the quasars is shown in Fig. 6, where an excess of absorbers up to tens of thousands of km s^{-1} is visible. They conclude that (i) quasars destroy Mg II and C IV absorbers to the distances of 800 and 300 kpc respectively, (ii) 40% of the absorbers within 3000 km s^{-1} can not be accounted for by clustering alone, and are intrinsic to the quasars, and (iii) intrinsic absorbers extend to relative velocities of $12,000 \text{ km s}^{-1}$. Nestor, Hamman & Rodriguez Hindalgo (2008) have drawn similar conclusions from a study C IV systems in SDSS DR4.

4.6 Chemical enrichment of the Universe

As noted above, most of the neutral gas in the Universe is believed to reside in DLAs. These systems have an advantage over other type of systems for abundance measurement as, due to

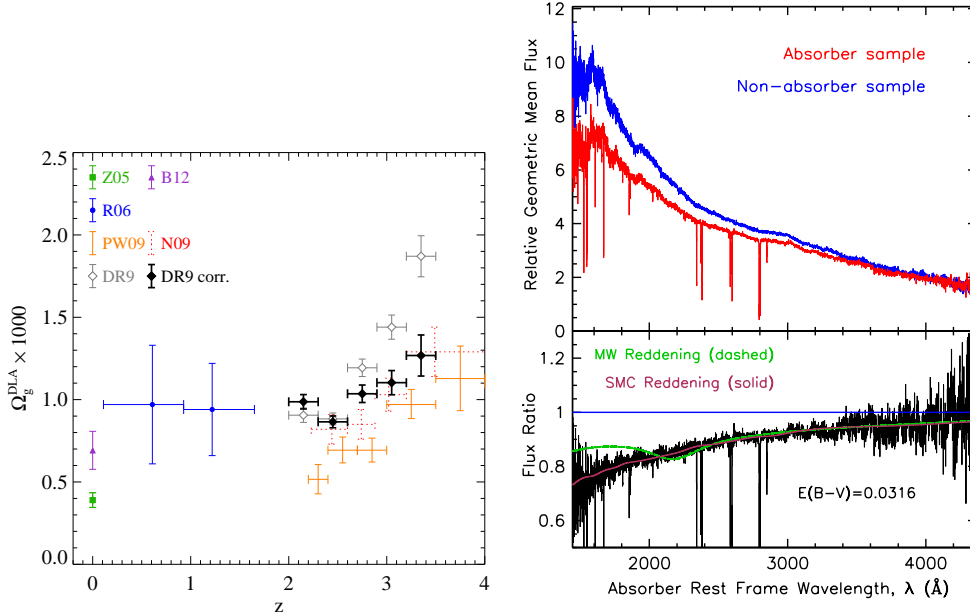


Figure 5. Left Panel : Cosmological mass density of neutral gas in DLAs as a function of redshift (Z05: Zwaan et al. 2005; B12: Braun 2012; R06: Rao et al. 2006; PW09: Prochaska & Wolfe 2009; DR9: Noterdaeme et al. 2012b). Courtesy Noterdaeme et al. (2012b) A&A, 547, L1. Right Panel: The top panel shows the geometric mean composite spectrum of the absorber sample of 251 intervening systems, having $W_{\text{Mg II}} > 2.5 \text{ \AA}$ (red curve), and that of the corresponding non-absorbers (blue curve). The bottom panel shows the ratio of the two spectra along with the best fit SMC extinction curve as continuous maroon line. The derived absorber rest-frame $E(B - V)$ value is given. The MW extinction curve for the derived SMC $E(B - V)$ value is shown as dashed green line. Courtesy York et al. (2006), MNRAS, 367, 945.

their high H I column density, the ionization corrections are expected to be small. The chemical enrichment history of the Universe can, therefore, be understood by measuring the abundances in DLAs as a function of redshift. Being one of the least depleted elements, zinc is ideally used to measure abundances in DLAs.

Kulkarni et al. (2010), compiled samples of Zn and/or S abundances in 154 DLAs and 58 sub-DLAs, covering redshift range of 0.1-3.9. The global H I weighted mean metallicity for binned data for DLAs and sub-DLAs is shown in the left panel of Fig. 7 as a function of redshift. The metallicity of DLAs shows a weak evolution and does not rise to the expected solar values at the lowest redshifts which is in contrast to the predictions of theoretical models of chemical evolution, also plotted in the figure. The metallicity of sub-DLAs, however, rises more rapidly, and reaches solar values at redshifts < 1.0 . Several sub-DLAs were found to have near solar and super-solar abundances e.g. Khare et al. (2004), Meiring et al. (2009).

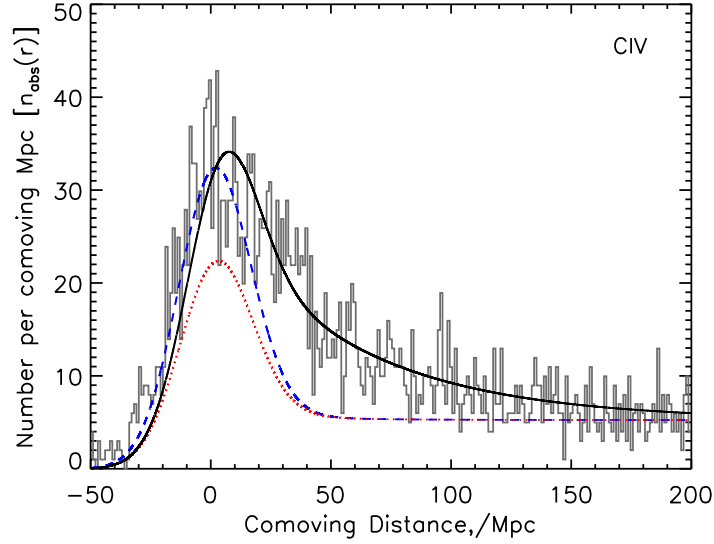


Figure 6. The number of C IV absorbers as a function of relative velocity with respect to quasars, expressed here in terms of the line-of-sight comoving distance from the quasar. The dashed line is the modeled galaxy clustering component, assuming the quasar photo-evaporates a sphere of radius 0.18 Mpc, smaller than the observed size of C IV halos at low redshift. The continuous line is for the full model including the intrinsic, out-flowing absorber distribution. The dotted line is the clustering component of this final model. Courtesy Wild et al. (2008), MNRAS, 388, 227.

Recently, Simcoe et al. (2012) have identified the lowest metallicity gas at a redshift of 7.04 (when the Universe was < 0.8 billion years old) in the spectrum of a quasar at $z_{\text{em}} = 7.08$ with $\log(N_{\text{HI}}) > 20.45$. Their upper limit to the metallicity is 10^{-4} times solar metallicity if the gas resides in a gravitationally bound protogalaxy, which is significantly lower than the lowest abundance observed so far.

4.7 Nature of DLA and sub-DLA absorbers

DLAs have been suggested to be the high redshift analogs of disks of nearby luminous galaxies. However, as noted in the previous section, they have been found to be metal poor even at redshifts close to zero. The metallicities of individual absorbers available in the literature, as well as the average metallicities for large samples of Mg II absorbers as determined by York et al. (2006), are plotted in the right panel of Fig. 7 as a function N_{HI} . The observed trend of decrease in metallicity with increase in N_{HI} has been attributed to selection effects (e.g. Boisse et al. 1998); the absence of high metallicity-high N_{HI} DLAs being due to their high dust column which may be rendering background quasars extinct.

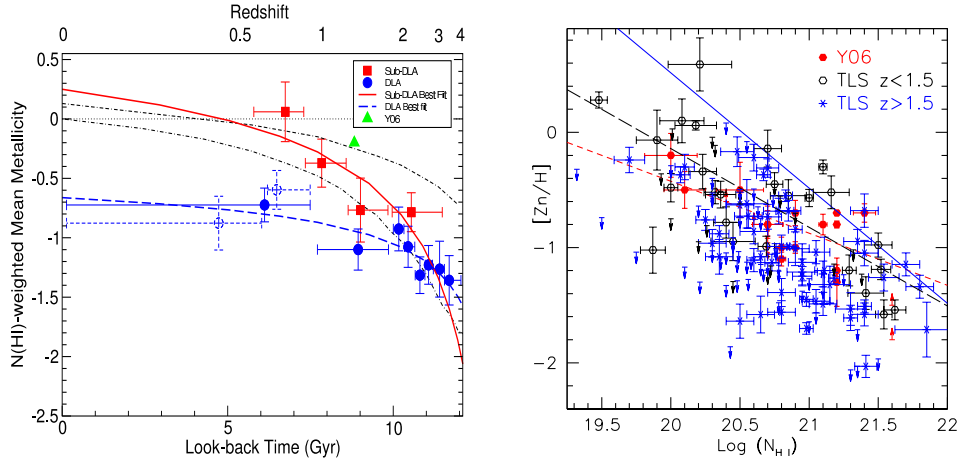


Figure 7. Left Panel: Logarithmic $N_{\text{H I}}$ -weighted mean Zn metallicity plotted vs. look-back time for DLAs and sub-DLAs. Dashed circles refer to the lowest time bin split into two bins with 10 DLAs each. The triangle denotes the formal lower limit to the average $[Zn/H]$ for a composite spectrum from 698 absorbers with average $\log(N_{\text{H I}}) \sim 20$ from York et al. (2006), referred to here as Y06. The curves show the mean metallicities in some of the chemical evolution models from literature. Courtesy Kulkarni et al. (2010) *New Astronomy*, 15, 735. Right Panel: Metallicity ($[Zn/H]$) vs. $\log(N_{\text{H I}})$. Solid circles represent average values for large samples as obtained by Y06. Open circles and stars are for redshifts < 1.5 and redshifts > 1.5 , respectively, for sample from the literature, referred to as TLS. One σ error bars are shown. Also shown are the best fit lines (long dashed line and short dashed line for the literature sample and the sample of Y06, respectively) obtained by ignoring the limits. The top solid line represents the empirical obscuration bias ($N_{\text{Zn II}} = 1.4 \times 10^{13} \text{ cm}^{-2}$). Courtesy Khare et al. (2007), *A&A*, 464, 487.

Khare et al. (2007), have argued that the amount of dust in quasar absorbers is small and can not be responsible for missing many quasars in magnitude limited surveys. While a bimodal dust distribution with a population of very dusty, metal rich, absorbers which push the background quasars below the observational threshold of available optical spectroscopic studies cannot be ruled out, observations indicate that the metallicity in quasar absorbers indeed decreases with increase in H I column densities beyond 10^{19} cm^{-2} . Misawa, Charleton & Narayanan (2008) have suggested an extension of the anticorrelation between metallicity and $N_{\text{H I}}$ to weak Mg II absorbers as well. Invoking the observed mass-metallicity relation for galaxies, Khare et al (2007) suggested that most sub-DLAs are associated with massive spiral/elliptical galaxies while most DLAs are associated with low mass galaxies. Ledoux et al. (2006) found a correlation between DLA metallicity and line profile velocity width, which is detected at the 6.1σ significance level over more than a factor of 100 spread in metallicity. This could be due to the mass-metallicity relation of absorbing galaxies.

Imaging studies of galaxies responsible for quasar absorption line systems (e.g. Bergeron & Boisse 1991; Peroux et al. 2012) have identified fewer than 60 galaxies out to ~ 50 kpc. These studies are ambiguous on the morphology of DLA and sub-DLA galaxies. Several absorbing

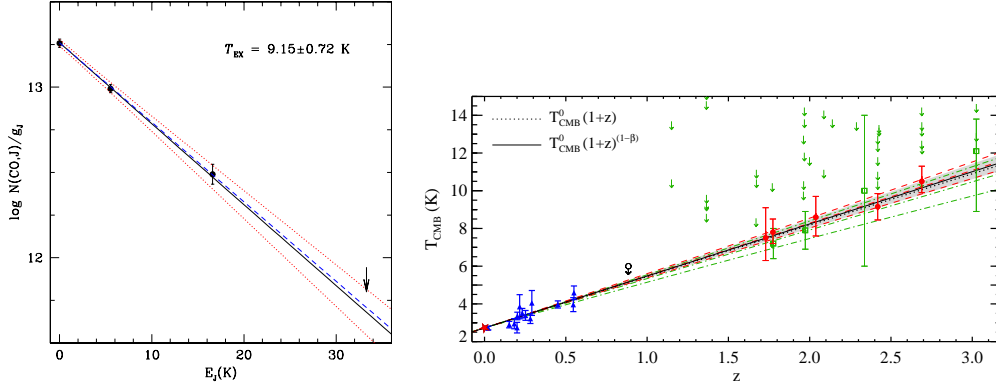


Figure 8. Left Panel: The CO excitation diagram. A straight line fit with slope $1/(T_{ex} \ln 10)$ indicates thermalization of the levels. The three lines give the mean and 1σ range obtained from T_{01} , T_{02} , and T_{12} . The diagram is compatible with thermalization by a black-body radiation of temperature 9.15 ± 0.72 K when $T_{\text{CMBR}} = 9.315 \pm 0.007$ K (long dashed line) is expected at the redshift of the absorption system (2.4185) from the hot big bang theory. Courtesy Srianand et al. (2008b) A&A, 482, L39. Right Panel: Measurements of T_{CMBR} at various redshifts. Measurements from CO are shown in red. Rest of the measurements use other methods. Dotted line shows prediction of the big bang model. Courtesy Noterdaeme et al. (2011), A&A, 526, L7.

galaxies have also been detected at high redshifts ($z > 2$) e.g. Moller et al. (2002); Noterdaeme et al. (2012a).

4.8 Molecules in quasar absorbers

Molecular gas is widely observed in the Milky Way. However, molecular hydrogen is scarce in QSOALS. In a survey consisting of observations of 77 DLA/strong sub-DLA systems, H_2 was found in only 13 ($\sim 17\%$) systems; in the rest of the systems the fraction of H_2 was found to be $< 10^{-5}$ (Noterdaeme et al. 2008a). Other molecules like HD, CO, HCO, HCN, HNC etc have been detected in a few absorbers (e.g. Wiklind & Combes 1996; Noterdaeme et al. 2008b; Noterdaeme et al. 2011). Detailed studies of molecular absorption give important information about the physical conditions in the absorbers as discussed below. Diffuse bands have been observed in one absorption system ($z_{\text{abs}} \approx 0.079$) for which galactic emission lines were detected in the SDSS spectra (Srianand et al. 2013).

5. Temperature of cosmic microwave background radiation at high redshifts

The big bang theory predicts an increase in the temperature of the CMBR, T_{CMBR} , with redshift, as $(1+z)$. Srianand et al. (2008b) have determined T_{CMBR} in a sub-DLA absorber at $z_{\text{abs}} = 2.42$ in

SDSS J143912.04+111740.5. They measured column densities of H I, C I, H₂, and CO in ground and excited levels. The measured column densities of CO in 3 rotational levels are plotted in the left panel of Fig. 8, which shows that the populations are well thermalized. From the analysis of populations of C I and H₂ in their ground and excited levels they determined constraints on physical conditions namely, the particle density and temperature, in the absorber and concluded that the collisional excitations of rotational levels of CO is negligible. The populations of excited levels of CO are then determined by radiation pumping by the CMBR and yield $T_{\text{CMBR}} = 9.15 \pm 0.72$ K which is consistent with the expectations of the big bang model. CO has been observed in five systems so far in sufficient details so as to estimate T_{CMBR} at the redshifts of these systems. Combining these data with the T_{CMBR} obtained using other techniques, Noterdaeme et al. (2011) have shown that its redshift dependence can be expressed as $T_{\text{CMBR}}(z) = T_{\text{CMBR}}(0)(1+z)^{(1-\beta)}$, with $\beta = -0.007 \pm 0.027$ and is consistent with the standard big bang model.

6. Time variability of fundamental constants

Contemporary theories of fundamental interactions allow the fundamental constants to vary as a function of space and time. Therefore, direct measurements of possible time variations of various fundamental quantities are of utmost importance for a complete understanding of fundamental physics. At redshifts >0 , a possible time dependence of the fine structure constant, α , can be seen in the form of small shifts in the wavelengths of quasar absorption lines, as energies of the atomic and molecular transitions depend on α . Murphy, Webb & Flambaum (2003) studied a sample of 128 systems observed with HIRES at KECK telescope. Using many multiplet analysis, they obtained $\Delta\alpha/\alpha = (-0.574 \pm 0.102) \times 10^{-5}$, over redshift range of 0.2-3.7, implying a 5σ variation. Srianand et al. (2004), used an independent sample of 23 systems observed with VLT-UVES at high signal to noise ratio, covering redshift between 0.4 and 2.3. Using strict selection criterion in order to improve the sensitivity of the results, they obtained $\Delta\alpha/\alpha = (-0.06 \pm 0.06) \times 10^{-5}$, ruling out any variation of α . Webb et al. (2011) analyzed 153 systems to show that at $z < 1.8$, $\Delta\alpha/\alpha = (-0.6 \pm 1.6) \times 10^{-6}$. However, combining their VLT and KECK data, they find a spatial variation of α and suggest existence of an α -dipole. Rahmani et al. (2012), using optical and radio observations, have determined constraints on the time variation of $x = g_p \alpha^2 / \mu$, where g_p is the proton gyromagnetic factor and μ is the proton to electron mass ratio, at $1.17 < z < 1.56$, using optical and radio observations. No variation was found with $\Delta x/x = -(0.1 \pm 1.3) \times 10^{-6}$. Assuming constancy of other constants, they find $\Delta\alpha/\alpha = (0.0 \pm 0.8) \times 10^{-6}$.

Making use of the different dependence of wavelengths of inversion lines of NH₃ and rotational lines of CS and H₂CO molecules on the proton-to-electron mass ratio, μ , Kanekar (2011) has determined its variation from radio observations of an absorption system at $z = 0.685$. He finds the variation in μ over 6.2 Gyr to be $\Delta\mu/\mu = (-3.5 \pm 1.2) \times 10^{-7}$.

7. Future prospects

Above, I have tried to summarize some of the recent results obtained from the study of quasar absorption line systems. This field of research has completed almost 50 years as the absorption lines were discovered soon after the discovery of the quasars themselves. Initial progress in the

field was rather slow as the spectra had to be obtained on photographic plates and analysis was tedious. Also, the measurements could not be done to high accuracy on these spectra. The advent of CCDs and consequent digitization of the spectra, the development of Echelle spectrograph and of sophisticated image processing softwares e.g. IRAF, the commissioning of large telescopes e.g. KECK, VLT and Subaru and the launch of space telescopes covering various wavelength bands e.g. HST, Spitzer, Chandra, etc has launched a Tsunami of data on QSOALS and related fields. Simultaneously, availability of large computing powers has enabled astronomers and cosmologists to develop hydro simulation codes which can study structure formation and evolution on scales relevant to the observations. This has enabled the study of dependence of QSOALS properties on the cosmological parameters which are getting determined to high precision with CMB and supernova data.

With the planned large telescopes like the thirty metre telescope and the extremely large telescope in the optical, the Square Kilometer Array in the radio and James Webb telescope in the UV, the observational capability will reach unprecedented levels and it will be possible to observe QSOALS at higher redshifts and towards fainter quasars. The computing power is likely to improve simultaneously which will enable cosmological simulations on smaller and smaller space-time scales. Both these aspects will help solve the mystery of the quasar absorbers and yield a better understanding of the epoch of reionization, the chemical enrichment of the IGM and galaxies, quasar-absorbing galaxy connection at higher redshifts, missing baryon problem, the missing metal problem, quasar environment and dynamical effects therein, power spectrum of density fluctuations using the Ly α data etc.

References

- Adelberger K. L., 2005, in Williams P. R., Shu C., Menard, B., eds, Probing galaxies through quasar absorption lines, P. 341
- Allen J. T., Hewett P., C., Maddox N., Richards G. T., Belokurov V., 2011, MNRAS, 410, 860
- Bahcall J. N., Spitzer L., 1969, ApJ, 156, L63
- Bajtlik S., Duncan R. C., Ostriker J. P., 1988, ApJ, 327, 570
- Becker G. D., Hewett P. C., Worseck G., Prochaska J. X., 2013, MNRAS (in press); arXiv:1208.2584
- Bergeron J., Boisse P., 1991, A&A, 243, 344
- Bergeron J., 1988, in Blades J. C., Turnshek D. A., Norman C. A., eds, QSO absorption lines: Probing the Universe, Cambridge University Press, p. 275
- Bi H., Davidson A. F., 1997, ApJ, 479, 523
- Boisse P., Le Brun V., Bergeron J., Deharveng J. M., 1998, A&A, 333, 841
- Braun R., 2012, ApJ, 749, 87
- Calverley A. P., Beecker G. D., Haehnelt M. G., Bolton J. S., 2011, MNRAS, 412, 2543
- Cen R., Kang H., Ostriker J. P., Ryu D., 1995, ApJ, 451, 436
- Chen H.-W., Helsby J. E., Gauthier J.-R., Shectman S. A., Thompson I. B., Tinke, J. L., 2010, ApJ, 714, 1521
- Cooksey K. L., Kao M. M., Simcoe R. A., O'Meera J. M., Prochaska J. X., 2013, ApJ (in press), arXiv:1204.2827
- Cowie L. L., Songaila A., Kim T.-S., Hu E. M., 1995, AJ, 109, 1522
- Das S., Khare P., 1999, ApJ, 510, 597
- Dawson K. S., Schlegel D. J., Ahn C. P., et al., 2013, AJ, 145, 10

- Gabor W., et al., 2011, *ApJ*, 733, 24
Gallagher S. C., et al., 2006, *ApJ*, 644, 709
Gunn J. E., Peterson B. A., 1965, *ApJ*, 142, 1633
Jakobsen P., Boksenberg A., Deharveng P., Jedrzewski R., Paresce F., 1994, *Nature*, 370, 35
Jakobsen P., Jansen R. A., Wagner S., Reimers D., 2003, *A&A*, 397, 891
Jena T., Norman M. L., Tytler D., et al., 2005, *MNRAS*, 361, 70
Jiang P., Ge J., Zhou H., Wang J., Wang T., 2011, *ApJ*, 732, 110
Kanekar N., 2011, *ApJ*, 728, L12
Khare P., Kulkarni V. P., Lauroesch J. T., York D. G., Crotts A. P. S. & Nakamura O., 2004, *ApJ*, 675, 1002
Khare P., Kulkarni V. P., Peroux C., York D. G., Lauroesch J. T., Meiring J. D., 2007, *A&A*, 464, 487
Khare P., Vanden Berk D., York D. G., Lundgren B., Kulkarni V. P., 2012, *MNRAS*, 419, 1028
Khare P. et al. 2013, in preparation
Kirkman D., Tytler D., Lubin D., Charlton J., 2007, *MNRAS*, 376, 1227
Kirkman D., Tytler D., 2008, *MNRAS*, 391, 1457
Komatsu E., et al., 2011, *ApJS*, 192, 18
Kulkarni V. P., Khare P., Som D., Meiring J., York D. G., Peroux C., Lauroesch J. T., 2010, *New Astronomy*, 15, 735
Lanzetta K. M., Bowen D. V., Tytler D., Webb J. K., 1995, *ApJ*, 442, 538
Ledoux C., Petitjean P., Fynbo J. P. U., Moller P., Srianand R., 2006, *A&A*, 457, 71
Loeb A., Eisenstein D. J., 1995, *ApJ*, 448, 17
Lu, Y., Yu Q., 2011, *ApJ*, 736, 49
Matejek M. S., Simcoe R. A., Cooksey K. L., Seyffert E. N., 2013, *ApJ*, 764, 9
Meiksin A. A., 1994, *ApJ*, 431, 109
Meiksin A. A., 2009, *Rev. Modern Physics*, 81, 1405
Meiring J. D., Lauroesch J. T., Kulkarni V. P., Peroux C., Khare P., York D. G., 2009, *MNRAS*, 397, 2037
Menard B., Wild V., Nestor D., Quider A., Zibetti S., Rao S., Turnshek D., 2011, *MNRAS*, 417, 801
Misawa T. Charlton J. C., Narayanan A., 2008, *ApJ*, 679, 220
Mo H. J., Morrison S. L., 1994, *MNRAS*, 269, 52
Mo H. J., Miralda-Escude J., 1996, *ApJ*, 469, 589
Moller P., et al., 2002, *A&A*, 396, 21
Mortlock D. J., et al., 2011, *Nature*, 474, 616
Murphy M. T., Webb J. K., Flambaum V. V., 2003, *MNRAS*, 345, 609
Murphy M. T., Liske J., 2004, *MNRAS*, 354, L31
Murphy M. T., Webb J. K., Flambaum V. V., 2008, *MNRAS*, 384, 1053
Muzahid S., Srianand R., Bergeron J., Petitjean P., 2012, *MNRAS*, 421, 446
Nestor D. B., Rao S. M., Turnshek D. A., Vanden Berk D., 2003, *ApJ*, 595, L5
Nestor D. B., Turnshek D. A., Rao S. M., 2005, *ApJ*, 628, 637
Nestor D. B., Hamann F., Rodriguez Hidalgo P., 2008, *MNRAS*, 386, 2055
Noterdaeme P., Ledoux C., Petitjean P., Srianand R., 2008a, *A&A*, 481, 327
Noterdaeme P., Petitjean P., Ledoux C., Srianand R., Ivanchik A., 2008b, *A&A*, 491, 397
Noterdaeme P., Petitjean P., Ledoux C., Srianand R., 2009, *A&A*, 505, 1087
Noterdaeme P., Srianand R., Mohan V., 2010, *MNRAS*, 403, 906
Noterdaeme P., Petitjean P., Srianand R., Ledoux C., Lopez S., 2011, *A&A*, 526, L7
Noterdaeme P., et al., 2012a, *A&A*, 540, 63
Noterdaeme P., et al., 2012b, *A&A*, 547, L1
Paschos P., Jena T., Tytler D., Kirkman D., Norman M. J., 2009, *MNRAS*, 399, 1934
Pei Y. C., Fall S. M., Bechtold J., 1991, *ApJ*, 378, 6
Peroux C., Bouche N., Kulkarni V. P., York D. G., Vladillo G., 2012, *MNRAS*, 419, 3060

- Prochaska J. X., Herbert-Fort S., Wolfe A. M., 2005, *ApJ*, 635, 123
- Prochaska J. X., Hennawi J. F., Herbert-Fort S., 2008, *ApJ*, 675, 1002
- Prochaska J. X., Wolfe, Arthur A. M., 2009, *ApJ*, 696, 1543
- Prochaska J. X., Weiner B., Chen H.-W., Mulchaey J., Cooksey K., 2011, *ApJ*, 740, 91
- Quider A. M., Nestor D. B., Turnshek D. A., Rao S. M., Monier E. M., Weyant A. M., Busche J. R., 2011, *AJ*, 141, 137
- Rahmani H., Srianand R., Gupta N., Petitjean P., Noterdaeme P., Albornoz Vasquez D., 2012, *MNRAS*, 425, 556
- Rao S., Turnshek D. A., 2000, *ApJS*, 130, 1
- Rao S., Turnshek D. A., Nestor, D. B., 2006, *ApJ*, 636, 610
- Rauch M., 1998, *ARAA*, 36, 267
- Rees M. J., 1986, *MNRAS*, 218, 25
- Rollinde E., Srianand R., Theuns T., Petitjean P., Chand H., 2005, *MNRAS*, 361, 1015
- Sargent W. L. W., Young P. J., Bokserberg A., Tytler D., 1980, *ApJS*, 42, 41
- Schroeder J., Messinger A., Heiman Z., 2013, *MNRAS*, 428, 3058
- Shull J. M., Tumlinson J., Giroux M. L., Kriss, G. A., Reimers D., 2004, *ApJ*, 600, 570
- Shull J. M., Smith B. D., Danforth C. W., 2012, *ApJ*, 759, 23
- Simcoe R. A., 2011, *ApJ*, 738, 159
- Simcoe R. A., Sullivan P. W., Cooksey K. L., Kao M. M., Matejek M. S., Burgasser A. J., 2012, *Nature*, 492, 79
- Srianand R., Chand H., Petitjean P., Aracil B., 2004, *PRL*, 92, 121302
- Srianand R., Gupta N., Petitjean P., Noterdaeme P., Saikia D. J., 2008a, *MNRAS*, 391, 69
- Srianand R., Noterdaeme P., Ledoux C., Petitjean P., 2008b, *A&A*, 482, L39
- Srianand R., Gupta N., Rahmani H., Momjian E., Petitjean P., Noterdaeme P., 2013, *MNRAS*, 428, 2198
- Steidel C. C., Sargent W. L. W., 1989, *ApJS*, 69, 703
- Steidel C. C., Sargent W. L. W., 1992, *ApJS*, 80, 1
- Tejos N., Morris S. L., Crighton N. H. M., Theuns T., Altye G., Finn C. W., et al., 2012, *MNRAS*, 425, 245
- Tripp T. M., Savage B. D., Jenkins E. B., 2000, *ApJ*, 534, L1
- Tripp T. M., 2013, arXiv:1303.0043
- Vandenberk D. E., et al., 1996, *ApJ*, 469, 78
- Vanden Berk D., Khare P., York D. G., et al., 2008, *ApJ*, 679, 239
- Vivek M., Srianand R., Mahabal A., Kuriakose V. C., 2012, *MNRAS*, 421, L107
- Wang B., 1995, *ApJ*, 444, L17
- Webb J. K., King J. A., Murphy M. T., Flambaum V. V., Carswell R. F., Bainbridge M. B., 2011, *PhRvL*, 107, 1101
- Weyman R. J., Williams R. E., Peterson B. M., Turnshek D. A., 1979, *ApJ*, 234, 33
- Weyman R. J., Carswell R. F., Smith M. G., 1981, *ARA&A*, 19, 41
- Wild V., Hewitt P. C., 2005, *MNRAS*, 361, 30
- Wild V., Kauffmann G., White S., et al., 2008, *MNRAS*, 388, 227
- Wiklind T., Combes F., 1996, *A&A*, 315, 86
- Wolfe A. M. E., Gawiser E., Prochaska J. X., 2005, *ARAA*, 43, 861
- Wyithe J. S. B., Loeb A., 2003, *ApJ*, 586, 693
- York D. G., Yanny B., Crofts A., et al., 1991, *MNRAS*, 250, 24
- York D. G., et al., 2000, *AJ*, 120, 1579
- York D. G., Khare P., Vanden Berk, D., et al., 2006, *MNRAS*, 367, 945
- Zibetti S., Menard B., Nestor D., Turnshek D., 2005, *ApJ*, 631, L105
- Zwaan M. A., van der Hulst J. M., Briggs F. H., Verheijen M. A. W., Ryan-Weber E. V., 2005, *MNRAS*, 364, 1467